ACS Catalysis

Letter

pubs.acs.org/acscatalysis

Unraveling the Mechanism of the Cinchoninium Ion Asymmetric Phase-Transfer-Catalyzed Alkylation Reaction

Ernane de Freitas Martins and Josefredo Rodriguez Pliego, Jr.*

Departamento de Ciências Naturais, Universidade Federal de São João del-Rei 36301-160, São João del-Rei, MG, Brazil

Supporting Information

ABSTRACT: The mechanism of the alkylation reaction of the indanone anion through asymmetric phase-transfer catalysis has been unraveled by density functional theory calculations. Our results point out that the present view of the asymmetry induction mechanism determined by hydrogen bond and $\pi-\pi$ stacking interactions is not correct. Rather, stabilization of the main reaction pathway takes place through both the hydrogen bond and electrostatic interaction involving the leaving chloride anion.

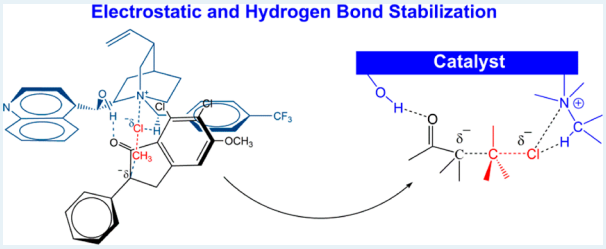

KEYWORDS: *alkylation, asymmetric catalysis, organocatalysis, density functional calculations, hydrogen bond, phase-transfer catalysis*

Controlling the stereochemistry of chemical reactions through asymmetric catalysis has become a fascinating area of research.[1−5] In this respect, phase-transfer catalysis has been particularly explored in recent years[6−10] because it is considered a green chemistry procedure[11,12] and its chiral version is useful for the synthesis of pharmaceuticals.[13−15] Among these catalysts, cinchona alkaloid derivatives have particulary attracted a lot of interest because they are natural products and are considered privileged chiral catalysts.[16−19]

Almost 30 years ago, Dolling and co-workers reported for the first time a highly enantioselective reaction promoted by phase-transfer catalysis.[20,21] Methylation of 6,7-dichloro-5-methoxy-2-phenyl-1-indanone (**1**) was shown to yield (*S*)-(+)-6,7-dichloro-5-methoxy-2-methyl-2-phenyl-1-indanone (**2**) in the presence of *N*-(*p*-(trifluoromethyl)benzyl)cinchoninium bromide (**3**) acting as a phase-transfer catalyst (Scheme 1). These findings were rationalized on the basis of the interaction of the cinchoninium cation with the indanone anion and the stabilization of the ion-pair structure by hydrogen bonding and $\pi-\pi$ stacking interactions (Scheme 2).

Scheme 1. Phase-Transfer-Catalyzed Alkylation of Indanone 1 through Catalyst 3

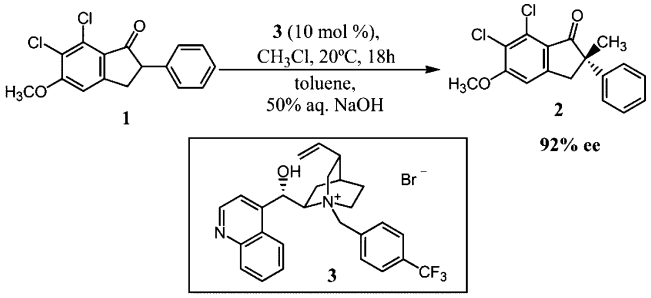

Scheme 2. The Dolling et al. Proposal[a] and the Corey Proposal[b]

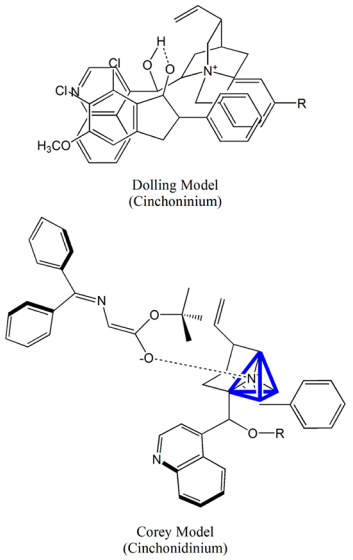

[a]Based on the interaction of the cinchoninium (**3**) with the deprotonated indanone (**1**). [b]Based on the interaction of the cinchonidinium with the anion.

A few years later, O'Donnell et al[22] showed that cinchona alkaloid derivatives could be used for the synthesis of amino acids by asymmetric catalysis, and in 1997, the Corey[23] and the Lygo[24] groups reported the application of new *N*-anthracenylmethyl-substituted cinchona alkaloid phase-transfer catalysts with increased activity for asymmetric-catalyzed amino acids

Received: January 9, 2013
Revised: February 25, 2013
Published: February 27, 2013

synthesis. Corey and co-workers[23] proposed that the asymmetry induction of the cinchonidinium cation was due to the interaction of the anionic oxygen of the nucleophile with the positively charged nitrogen atom of the catalyst involving only one side of an imaginary tetrahedron centered on nitrogen. Other positions were considered to be sterically less accessible (Scheme 2).

Although these cinchona-based phase-transfer catalysts are now widely used, a full understanding of the asymmetry induction mechanism remains obscure. This has led Denmark and co-workers to analyze this challenging problem in search of quantitative structure−activity and −selectivity relationships.[25−27] On the other hand, recent theoretical studies have provided some important new insights on phase-transfer catalysis.[28−33] Yet, the role of cinchona-based catalysts has received less theoretical attention, presumably because these systems are large and flexible, leading to more difficult and more computer-demanding calculations.[34] In this paper, we specifically address the role of this type of phase transfer catalyst and report results of theoretical calculations that provide a clear picture for the mechanism of asymmetry induction promoted by the cinchoninium cation in phase-transfer-catalyzed reactions. The theoretical results are based on DFT calculations with the X3LYP functional[35−37] and extended basis set,[38] which provides a good description of hydrogen bonds and van der Waals forces. Solvent effects were included through the PCM method.[39,40] The calculations were done with the Firefly[41] and GAMESS[42] programs. Details are presented in the Supporting Information.

In our model reaction (Scheme 1), the approach of a cinchoninium cation to the indanone anion is predicted to lead to the formation of a stable ion pair. Because of the relative torsional freedom of the cinchoninium cation, the most stable ion pair complex does not necessarily retain the lowest energy conformation of the isolated cation. Therefore, we tested several different structures for the anion−catalyst complex and found a total of 12 minima energy structures on the potential energy surface. From this set, structures MS6a and MS6b, shown in Figure 1, are predicted to be the most stable ones by at least 2 kcal/mol. Upon close observation of these structures, several important features emerge: (a) the −OH group of the catalyst makes a strong hydrogen bond with the carbonyl oxygen of the indanone anion (H···O distance around 1.6 Å); (b) the face of the tetrahedron centered on the N atom nearer the OH group corresponds to the side where the anion approaches the catalyst; and (c) neither structure exhibits $\pi-\pi$ stacking interaction. MS6a and MS6b are predicted to be essentially isoenergetic, with the MS6b structure calculated to be only 0.4 kcal mol^{-1} more stable than MS6a (see ΔG^* in Table 1). The two complexes differ from each other by 180° rotation of the anion moiety around the C═O axis. Further analysis of these structures suggests that there are four possible transition states for the alkylation reaction from these two complexes leading to both *R* and *S* enantiomers. The structures of the complexes and transition states are shown in Figure 1 and can be better visualized in the mol files included as Supporting Information.

The calculated thermodynamic data for the relevant species are presented in Table 1. Transition states TS6a1 and TS6a2 correspond to alkylation on both sides of the indanone in the MS6a complex, leading to the *R* and *S* isomers, respectively. Likewise, transition states TS6b1 and TS6b2 lead to alkylation on both sides of the indanone in the MS6b complex, resulting

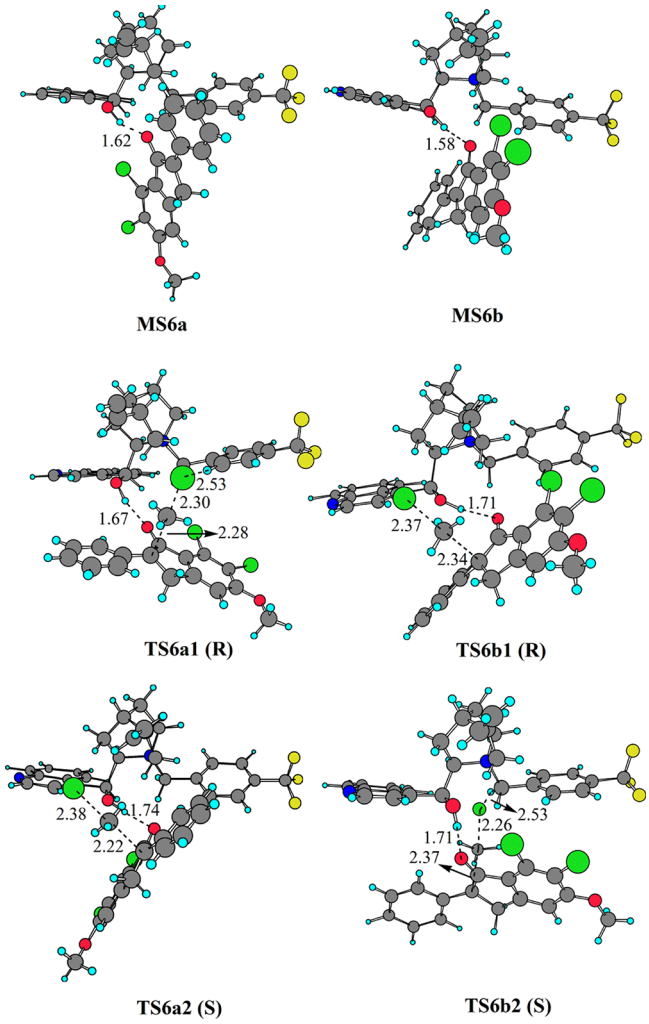

Figure 1. Optimized structures for the indanone−catalyst complexes (MS6a and MS6b) and the transition states (TS6a1, TS6a2, TS6b1, TS6b2).

in the *R* and *S* isomers, respectively. The activation free energies for all transition states were calculated with respect to the free energies of the MS6b isomer plus the free CH_3Cl species that were considered as our reference points. These calculations point out that TS6a2 and TS6b1 represent pathways of high activation barriers, both in excess of 30 kcal mol^{-1}. Thus, these pathways are deemed not to be kinetically important. By comparison, the TS6a1 and TS6b2 structures are much more stable, with $\Delta G^{\ddagger}$ barriers of 27.6 and 26.1 kcal/mol, respectively. These transition states can then be proposed to be responsible for the observed reaction rate and to explain the enantiomeric excess (ee). In fact, the 1.5 kcal mol^{-1} difference in our calculated $\Delta G^{\ddagger}$ leads to an ee of 86% in favor of the *S* enantiomer at 20 °C, a value that is in very good agreement with the experimental result of 92%.[20] Although DFT calculations are more accurate for relative barriers than for absolute barriers, we should bear in mind that there is some uncertainty in the calculated free energies.

The origin of the enantioselectivity can be understood by analyzing the structures shown in Figure 1. The relative stabilization of the transition states is expected to depend on electrostatic interactions and, thus, on the distance between the departing negative charged chloride anion and the positively charged nitrogen center of the cinchoninium cation. These

dx.doi.org/10.1021/cs400021r | *ACS Catal.* 2013, 3, 613−616

Table 1. Relative Stability of the MS6a Isomer and Transition States with Respect to MS6b[a]

	X3LYP/6-31(+)G(d)	X3LYP/TZVPP+diff	$\Delta G_g{}^{*b}$	$\Delta\Delta G_{solv}{}^{c}$	$\Delta G_{sol}{}^{*d}$
MS6a	−0.86	−0.68	0.07	0.31	0.38
TS6a1	13.63	17.13	27.71	−0.15	27.56
TS6a2	20.41	22.30	33.75	−1.29	32.46
TS6b1	20.65	24.75	35.37	−1.81	33.56
TS6b2	10.74	13.88	25.15	0.95	26.10

[a]Units of kcal mol^{-1}. Standard state 1 mol L^{-1}. [b]Gas phase free energy. [c]Solvation contribution (toluene). [d]Solution phase free energy

distances amount to 5.78 and 6.12 Å, respectively, for the less stable transition states TS6a2 and TS6b1, whereas for the most stable TS6a1 and TS6b2 structures, the distances between the leaving chloride and the cinchoninium nitrogen atom are calculated to be 4.86 and 4.50 Å, respectively. Thus, there is a clear correlation between the Cl−N distance in the transition state and the $\Delta G^{\ddagger}$, as shown in Figure 2.

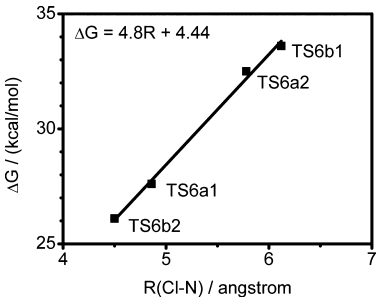

Figure 2. Linear relationship between the free energy of activation and the Cl−N distance in the transition state.

Another interesting feature related to the stabilization of the TS6a1 and TS6b2 transition states is the role of hydrogen bonding. Figure 1 shows that the leaving chloride anion in TS6a1 is hydrogen-bonded to one of the hydrogens of the $-C_6H_4CF_3$ group, with a H···Cl distance calculated to be 2.53 Å. Similarly, the TS6b2 structure displays hydrogen bonding between the leaving chloride anion and the hydrogen of the $N-CH_2-Ar$ group, with a H···Cl distance of 2.51 Å. By comparison, the less stable structures TS6a2 and TS6b1 do not exhibit these important hydrogen bonds. It is also worthwhile to observe that the anion−catalyst complexes found in our work correspond to very flexible structures, with some of the transition states displaying large distortions from the parent complex.

The role of the intermolecular forces responsible for the stabilization of transition state TS6b2 can be summarized with the help of Figure 3. The negative charge present in the carbonyl oxygen of the nucleophile interacts by hydrogen bonding with the hydroxyl group of the catalyst while the leaving chloride ion interacts with the center of positive charge in the catalyst. The closer the chloride anion is to the nitrogen atom in the transition state, the higher will be the stabilization conferred to the structure. It is worthwhile to notice that a similar concept was advanced by us[43,44] for anionic S_N2 reactions some years ago, leading to predictions regarding the preference for nucleophilic displacement over elimination.[45]

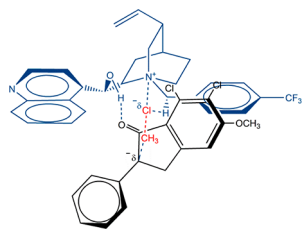

Figure 3. Interaction of the cinchoninium ion with the S_N2 transition state.

The present model is also superior to that of Dolling and co-workers for explaining the experimental observations. In fact, altering the methylating agent from methyl chloride to bromide and iodide leads to a decrease in the enantioselectivity.[21] In the Dolling model, there is no reason for this behavior, because in the transition state, there is only one side available for the reaction. In the present model, the transition state fits to the cation through hydrogen bond and electrostatic interaction. Thus, the nature of the leaving group is important because the halide−carbon distance in the transition state and the charge in development in the leaving halide play a key role in the stabilization of TS6a1 and TS6b2. In addition, we could also notice from Table 1 that the solvent effect destabilizes the TS6b2 structure and stabilizes the TS6a1 structure. As a consequence, more-polar solvents decrease the selectivity, in line with experimental observations.

In summary, the picture of catalysis provided by this study is quite different from the current model of asymmetric induction. Our theoretical study shows that the interaction of the indanone anion (1) with the cinchoninium cation (3) can yield 12 ion pair complexes through electrostatic and hydrogen bond interaction, but without evidence for $\pi-\pi$ stacking interaction. Two out of the 12 complexes are much more stable than the other structures and lead to four transition states. Our analysis shows that the free energy of activation of these four transition states bear a linear relationship with the distance of the leaving chloride to the nitrogen atom of the quinuclidine ring. The most stable transition state, TS6b2, leading to the *S* enantiomer, has the lowest chloride−nitrogen distance. The mechanism of asymmetric catalysis proposed in this paper should be valuable in the design of new catalysts.

■ ASSOCIATED CONTENT

Supporting Information

Details of the calculations and optimized geometries of the minima and transition state structures. MDL molfiles are also available. This material is available free of charge via the Internet at http://pubs.acs.org.

■ AUTHOR INFORMATION

Corresponding Author

*pliego@ufsj.edu.br.

Notes

The authors declare no competing financial interest.

dx.doi.org/10.1021/cs400021r | *ACS Catal.* 2013, 3, 613−616

■ ACKNOWLEDGMENTS

The authors are thankful for the support of the agencies CNPq, FAPEMIG, and CAPES. The authors are also grateful to Professor Jose M. Riveros for reading the manuscript and for the invaluable suggestions.

■ REFERENCES

(1) Blaser, H. U.; Spindler, F.; Studer, M. *Appl. Catal., A* **2001**, *221*, 119−143.
(2) Knowles, R. R.; Jacobsen, E. N. *Proc. Natl. Acad. Sci. U.S.A.* **2010**, *107*, 20678−20685.
(3) Peng, F.; Shao, Z. *J. Mol. Catal. A: Chem.* **2008**, *285*, 1−13.
(4) Allemann, C.; Gordillo, R.; Clemente, F. R.; Cheong, P. H. Y.; Houk, K. N. *Acc. Chem. Res.* **2004**, *37*, 558−569.
(5) DiRocco, D. A.; Noey, E. L.; Houk, K. N.; Rovis, T. *Angew. Chem., Int. Ed.* **2012**, *51*, 2391−2394.
(6) Albanese, D.; Landini, D.; Maia, A.; Penso, M. *J. Mol. Catal. A: Chem.* **1999**, *150*, 113−131.
(7) Starks, C. M., Phase-Transfer Catalysis: An Overview. In *Phase-Transfer Catalysis*; Starks, C. M., Ed.; American Chemical Society: Washington, DC, 1987.
(8) Ooi, T.; Maruoka, K. *Angew. Chem., Int. Ed.* **2007**, *46*, 4222−4266.
(9) Maruoka, K.; Ooi, T.; Kano, T. *Chem. Commun.* **2007**, 1487−1495.
(10) Hashimoto, T.; Maruoka, K. *Chem. Rev.* **2007**, *107*, 5656−5682.
(11) Makosza, M. *Pure Appl. Chem.* **2000**, *72*, 1399−1403.
(12) Maruoka, K. *Pure Appl. Chem.* **2012**, *84*, 1575−1585.
(13) Ikunaka, M. *Org. Process Res. Dev.* **2008**, *12*, 698−709.
(14) Maruoka, K. *Org. Process Res. Dev.* **2008**, *12*, 679−697.
(15) Hua, M.-Q.; Cui, H.-F.; Wang, L.; Nie, J.; Ma, J.-A. *Angew. Chem., Int. Ed.* **2010**, *49*, 2772−2776.
(16) Yoon, T. P.; Jacobsen, E. N. *Science* **2003**, *299*, 1691−1693.
(17) Jew, S. S.; Park, H. G. *Chem. Commun.* **2009**, 7090−7103.
(18) Maruoka, K.; Ooi, T. *Chem. Rev.* **2003**, *103*, 3013−3028.
(19) Tian, S.-K.; Chen, Y.; Hang, J.; Tang, L.; McDaid, P.; Deng, L. *Acc. Chem. Res.* **2004**, *37*, 621−631.
(20) Dolling, U. H.; Davis, P.; Grabowski, E. J. J. *J. Am. Chem. Soc.* **1984**, *106*, 446−447.
(21) Hughes, D. L.; Dolling, U. H.; Ryan, K. M.; Schoenewaldt, E. F.; Grabowski, E. J. J. *J. Org. Chem.* **1987**, *52*, 4745−4752.
(22) O'Donnell, M. J.; Bennett, W. D.; Wu, S. *J. Am. Chem. Soc.* **1989**, *111*, 2353−2355.
(23) Corey, E. J.; Xu, F.; Noe, M. C. *J. Am. Chem. Soc.* **1997**, *119*, 12414−12415.
(24) Lygo, B.; Wainwright, P. G. *Tetrahedron Lett.* **1997**, *38*, 8595−8598.
(25) Denmark, S. E.; Weintraub, R. C. *Heterocycles* **2011**, *82*, 1527.
(26) Denmark, S. E.; Gould, N. D.; Wolf, L. M. *J. Org. Chem.* **2011**, *76*, 4337−4357.
(27) Denmark, S. E.; Gould, N. D.; Wolf, L. M. *J. Org. Chem.* **2011**, *76*, 4260−4336.
(28) Benjamin, I. *J. Phys. Chem. B*, article ASAP, DOI: 10.1021/jp306669t.
(29) Nelson, K. V.; Benjamin, I. *J. Phys. Chem. C* **2011**, *115*, 2290−2296.
(30) Nelson, K. V.; Benjamin, I. *Chem. Phys. Lett.* **2010**, *492*, 220−225.
(31) Nelson, K. V.; Benjamin, I. *J. Phys. Chem. C* **2010**, *114*, 1154−1163.
(32) Pliego, J. R., Jr.; Riveros, J. M. *J. Mol. Catal. A: Chem.* **2012**, *363*−*364*, 489−494.
(33) Pliego, J. R., Jr.; Pilo-Veloso, D. *Phys. Chem. Chem. Phys.* **2008**, *10*, 1118−1124.
(34) Cheong, P. H.-Y.; Legault, C. Y.; Um, J. M.; Çelebi-Olçüm, N.; Houk, K. N. *Chem. Rev.* **2011**, *111*, 5042−5137.
(35) Xu, X.; Zhang, Q.; Muller, R. P.; Goddard Iii, W. A. *J. Chem. Phys.* **2005**, *122*, 014105−14.
(36) Xu, X.; Goddard, W. A., III. *Proc. Natl. Acad. Sci. U.S.A.* **2004**, *101*, 2673−2677.
(37) Su, J. T.; Xu, X.; Goddard, W. A., III. *J. Phys. Chem. A* **2004**, *108*, 10518−10526.
(38) Weigend, F.; Ahlrichs, R. *Phys. Chem. Chem. Phys.* **2005**, *7*, 3297−3305.
(39) Cances, E.; Mennucci, B.; Tomasi, J. *J. Chem. Phys.* **1997**, *107*, 3032−3041.
(40) Cossi, M.; Barone, V.; Cammi, R.; Tomasi, J. *Chem. Phys. Lett.* **1996**, *255*, 327−335.
(41) Granovsky, A. A. *Firefly*, version 7.1.F: 2009.
(42) Schmidt, M. W.; Baldridge, K. K.; Boatz, J. A.; Elbert, S. T.; Gordon, M. S.; Jensen, J. H.; Koseki, S.; Matsunaga, N.; Nguyen, K. A.; Su, S.; Windus, T. L.; Dupuis, M.; Montgomery, J. A., Jr. *J. Comput. Chem.* **1993**, *14*, 1347−1363.
(43) Pliego, J. R., Jr. *J. Phys. Chem. B* **2009**, *113*, 505−510.
(44) Pliego, J. R., Jr. *J. Mol. Catal. A: Chem.* **2005**, *239*, 228−234.
(45) Pliego, J. R., Jr. *Phys. Chem. Chem. Phys.* **2011**, *13*, 779−782.